

ARTICLES

Stereodynamics and Outer Valence Ionic States of Ferrocene in Collisional Ionization with a He*(2³S) Metastable Atom by Two-Dimensional Penning Ionization Electron Spectroscopy

Naoki Kishimoto and Koichi Ohno*

*Department of Chemistry, Graduate School of Science, Tohoku University, Aramaki, Aoba-ku, Sendai 980-8578, Japan**Received: June 18, 2008; Revised Manuscript Received: November 18, 2008*

Outer valence ionic states of ferrocene were investigated by means of Penning ionization electron spectroscopy upon collision with metastable He*(2³S) excited atoms. By two-dimensional measurement combining electron spectroscopy and collision-energy-resolved technique of the metastable atomic beam, ionic-state-resolved measurements of collision energy dependence of partial Penning ionization cross sections (CEDPICS) were carried out. Since the partial Penning ionization cross sections can be connected with spatial extension of corresponding molecular orbitals (MOs) outside the boundary surface for the collision with He* atoms, different slope values of CEDPICS were related with stereodynamics in Penning ionization as well as anisotropic interaction around the ionization region: attractive interaction around ligand π orbitals and repulsive interaction around ligand σ orbitals and the metal atom. The observed negative collision energy dependence of ionization cross sections for the first (²E₂') and second (²A₁') ionic states was consistent with configuration interactions suggested by ab initio MO calculations [*J. Chem. Phys.* **2002**, *117*, 6533], which is due to the strong electron correlation effects beyond the one-electron MO description.

I. Introduction

Ferrocene¹ [Fe(C₅H₅)₂] is a typical sandwich organometallic complex (metallocene), and its structure is stable by strong chemical bonding between a metal atom and cyclopentadienyl rings as known by the 18-electron rule. Electronic properties of organometallic compounds have attracted considerable interest, and the electronic structure of organometallic compounds has not been investigated well mainly due to strong electron correlation effects and high spin states.

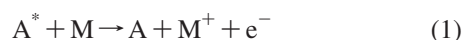
To investigate the electronic structure of organometallic compounds, electron spectroscopy methods and theoretical calculations of ionization energies have been utilized. Among

bis(cyclopentadienyl) metallic compounds, many metallocenes are open-shell molecules and it is difficult to calculate their ionic states, while ferrocene is a closed-shell molecule in the neutral ground state. Therefore, for the investigation of the observed ultraviolet photoelectron spectrum (UPS) of ferrocene,²⁻⁴ theoretical calculations of ionic states of ferrocene have been studied^{5,6} by post-Hartree–Fock methods taking electron correlation effects into consideration. It should be noted that the ionization energy order for ionization from 3d orbitals of Fe is considerably different from an ab initio Hartree–Fock calculation (Koopmans' theory), which is due to the importance of strong electron correlation effects and the breakdown of the one-to-one relationship between an MO and an ionic state. A high-level theoretical study by the cluster expansion configuration interaction calculation (SAC/SAC-CI)⁶ indicated that the first

* Corresponding author. E-mail: ohnok@qpcrkk.chem.tohoku.ac.jp.

two ionic states (${}^2E_2'$ and ${}^2A_1'$) have significant components of shake-up processes with configurations such as (${}^2E_2'$; $4e_1''-14e_2''-19e_1''+1$) or (${}^2A_1'$; $4e_1''-18a_1''-19e_1''+1$). A Green's functional method including electron correlation effects (ADC(3)) suggested many satellite bands in ionization potential energy more than 10 eV.⁵ Experimental assignments for the first four ionic states were suggested by photoelectron branching ratio and angle-resolved UPS^{7,8} to be (e_{2g} , a_{1g} , e_{1u} , and e_{1g}) ionization in D_{5d} symmetry representation.

Another measurement of ejected electrons for ionization of ferrocene is Penning ionization electron spectroscopy (PIES). By this method, orbital reactivity can be connected with spatial extension of molecular orbitals (MOs) outside of the boundary surface of a colliding excited rare gas atom A^* to a target molecule M ,⁹



since the transition probability for the electron transfer from an occupied MO of M to the inner singly occupied orbital of A^* depends mainly on the spatial overlap between the related orbitals. Reactivities of metal d orbitals of transition metal complexes such as ferrocene^{10,11} and other metallocenes¹² were found to be much smaller than those of ligand valence orbitals in the Penning ionization process, which means that metal d orbitals are shielded by ligands from the attack of the excited helium atoms. The shielding effect by ligands of metal complexes was also found for PIES of $Fe(CO)_5$ ¹³ and $M(CO)_6$ ($M = Cr, Mo, W$).¹⁴ In these studies, assignments of observed PIES bands were interpreted based on the one-electron picture for each ionic state by Koopmans' theorem. Thus, careful treatment would be necessary if one wishes to discuss the band intensity in PIES for organometallic compounds.

The change of orbital reactivity as a function of collision energy between metastable $He^*(2^3S)$ and ferrocene can be observed by a collision-energy-resolved technique of the metastable atomic beam. The two-dimensional (collision-energy/electron-energy-resolved) Penning ionization electron spectroscopy (2D-PIES)^{15,16} has enabled us to measure different collision energy dependence of partial ionization cross sections (CEDPICS)¹⁷ reflecting anisotropic interaction between $He^*(2^3S)$ and a target molecule. In addition, a different slope of CEDPICS for each ionic state can be valuable to determine the assignment of ionic states to related MOs. In this study, we have measured CEDPICS in Penning ionization of ferrocene, and the different slope values of CEDPICS can be connected to interaction around the metal d orbital region and the ligand valence orbital region. The strong electron correlation effects by shake-up ionization configurations on CEDPICS for the first and second ionic states are also interesting.

II. Methods

In our experimental setup,¹⁵⁻¹⁹ beams of electronically excited metastable $He^*(2^1,3S)$ atoms were produced by a nozzle discharge source with a tantalum hollow cathode.¹⁹ The $He^*(2^1S)$ component was eliminated by a water-cooled helium discharge lamp (quench lamp), and $He^*(2^3S)$ metastable atoms (19.82 eV) were led to the collision cell in the reaction chamber. He I UPS were measured by using the He I resonance photons (584 Å, 21.22 eV) produced by a discharge in pure helium gas. The background pressure in a reaction chamber was of the order of 10^{-7} Torr. Sample molecules were put in a sample cell set under the collision cell and vaporized under room temperature. The kinetic energy of ejected electrons was measured by a hemispherical electrostatic deflection type analyzer, using an

electron collection angle of 90° relative to the incident $He^*(2^3S)$ or photon beam. Measurement of the full width at half-maximum (fwhm) of the $Ar^+({}^2P_{3/2})$ peak in the He I UPS led to an estimate of 60 meV for the energy resolution of the electron energy analyzer. The transmission efficiency curve of the electron energy analyzer was determined by comparing our UPS data of some molecules with those by Gardner and Samson²⁰ and Kimura et al.²¹

In the experimental setup for the two-dimensional Penning ionization electron measurement, the metastable atom beam was modulated by a pseudorandom chopper,²² and then introduced into a reaction cell located at 504 mm downstream from the chopper disk. The measured Penning ionization spectra $I_e(E_e, t)$ were stored as a function of the electron kinetic energy (E_e) and time (t). The resolution of the analyzer was lowered to 250 meV to obtain higher counting rates of Penning electrons. Analysis of the time-dependent Penning ionization spectra by means of the Hadamard transformation²² and normalization by the velocity distribution of the He^* beam can lead to a two-dimensional mapping of the Penning ionization cross section [$\sigma(E_e, E_c)$] as functions of the electron energy, E_e , and collision energy, E_c . The velocity distribution of the metastable He^* beam was determined by monitoring secondary electrons emitted from a stainless steel plate inserted in the reaction cell. The experimental apparatus for $He^*(2^3S)$ 2D-PIES has been reported previously.^{16,18} For the CEDPICS, an appropriate range of E_c (typically fwhm of the band) was selected. The slope parameter (m) of CEDPICS was obtained by the least-squares method in the E_c range from ca. 100 to 300 meV.

To obtain electron density contour maps of MOs, we performed an SCF molecular orbital calculation. The geometry of ferrocene was selected from experimental studies.²³ In the electron density contour maps, thick solid curves indicate the repulsive molecular surface approximated by atomic spheres of van der Waals radii.²⁴ The value of radius for the Fe (2.04 Å) atom was estimated from half of the metal-metal bond lengths plus an empirical value of 0.8 Å, which is roughly the difference between the van der Waals radii and the single-bond covalent radii for several main group elements.²⁴ For the ionization potential energies, P3 propagator²⁵ calculation was performed with the GAUSSIAN 03 package program²⁶ with the 6-311+G* basis set.

On the basis of the well-known resemblance between $He^*(2^3S)$ and $Li(2^2S)$,^{27,28} a $Li(2^2S)$ atom in the ground state was utilized in place of a $He^*(2^3S)$ atom for potential surface calculations. This treatment enables us to avoid difficulties usually associated with ab initio MO calculations for highly excited states of a supermolecule consisting of a helium atom and an organometallic molecule. Interaction potentials between a $Li(2^2S)$ atom and the sample molecules were calculated by the density functional theory (DFT) with Becke's three-parameter exchange with the Lee, Young, and Parr correlation functional (B3LYP)²⁹ by using the 6-311+G* basis functions. The full counterpoise method³⁰ was used to correct the basis set superposition errors. The relaxation of the molecular frame geometry with a Li atom was confirmed to be very small.³¹

III. Results and Discussion

A. Ionization from Ligand π and σ Orbitals. Figure 1 shows He I UPS and $He^*(2^3S)$ PIES of ferrocene. Observed bands in UPS and PIES are labeled in numerical order as shown. Ionization bands 3, 5, and 7 can be assigned to cyclopentadienyl π orbitals (π_{Cp}) based on post-Hartree-Fock calculations listed in Table 1. Although the positions of band 5 in UPS and band

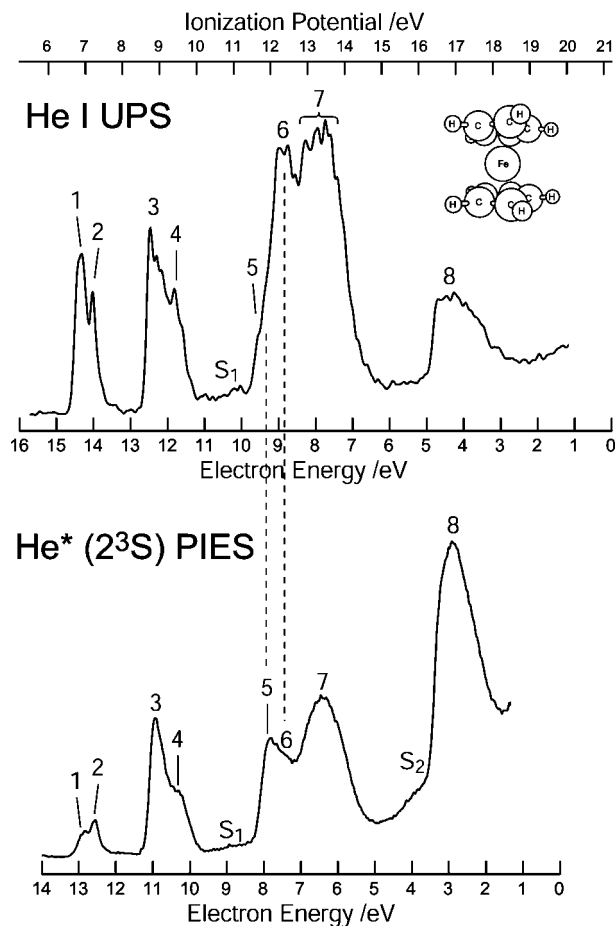


Figure 1. He I ultraviolet photoelectron spectrum (UPS) and He*(2^3S) Penning ionization electron spectrum (PIES) of ferrocene. S_1 and S_2 indicate satellite bands.

6 in PIES are not apparent, different character of UPS and PIES in band intensity enables us to determine the position of band 5 in PIES and band 6 in UPS complementally as shown by dotted lines in Figure 1. As described in the previous PIES studies,^{10–12} π_{Cp} bands show relatively large intensity rather than σ_{CH} band (band 6) in PIES, which can be ascribed to the spatially extending distribution of π_{Cp} orbitals as shown in Figure 2 and the electron exchange process³² of Penning ionization in which an electron of a target molecule transfers into the 1s orbital of He*(2^3S) and the excited electron is ejected to the continuum state simultaneously. Therefore, the transition probability mainly depends on spatial overlap between the target MO and the 1s orbital of He*, and an extending spatial distribution of an orbital results in large band intensity in PIES.^{9,17} Calculated IPs by Koopmans' theorem, P3 and ADC(3)⁵ methods, and SAC/SAC-CI theory⁶ are also listed in Table 1.

CEDPICS and collision-energy-resolved Penning ionization electron spectra (CERPIES) obtained from the 2D-PIES ($\sigma(E_c, E_e)$) are shown in Figures 2 and 3, respectively. For the CEDPICS, an appropriate range of E_e (typically fwhm of the band) was selected. Contour maps of electron densities for metal d and ligand valence MOs are also illustrated in Figure 2. Arrows in the figure indicate the most effective directions of collision. Fe and Cp in the figure indicate electron density maps on the planes at the Fe atom and 0.85 Å (equals half of the van der Waals radii²⁵ of C) above the Cp ring, respectively. The slope parameter (m) of CEDPICS was obtained by the least-squares method in the E_c range from ca. 100 to 300 meV, and listed in Table 1. For CERPIES, three spectra at collision

energies of 250, 170, and 100 meV are shown in Figure 3. In this figure, the intensity of bands 1–4 is shown 3 times as large as the original one. The negative slope of CEDPICS for π_{Cp} ionization bands can be ascribed to attractive interaction between the target molecule and He*(2^3S) atoms. It is known that slower He* atoms can penetrate into the reactive region more than the case of faster He* atoms because of the lower centrifugal barrier, which can lead to negative CEDPICS.^{16–18} When the attractive interaction of R^{-5} is dominant, ionization cross section $\sigma(E_c)$ can be expressed²⁸ by

$$\sigma(E_c) \propto E_c^{-2/5} \quad (2)$$

This formula was derived from the impact parameter at which orbiting occurs for atomic targets, and the slope of $\log \sigma(E_c)$ vs $\log E_c$ plot can be connected to the function form ($m = -2/5$). Indeed, an attractive potential well more than 100 meV was obtained for the model potential calculation for the access of Li to the π_{Cp} orbital region.

Interaction potential energy curves $V(R)$ as a function of the distance R between the Fe atom of ferrocene and a Li atom are shown in Figure 4. Repulsive interaction was calculated around the σ_{CH} orbital region, which is consistent with the smaller negative slope of CEDPICS for band 6 (σ_{CH} , $m = -0.15$) than that for band 3 (π_{Cp} , $m = -0.28$). In addition, the gentle negative slope of CEDPICS for the π_{Cp} bands (5 and 7) can be explained by the overlapping with σ_{CH} ionization bands in PIES. This may have a relationship with the interaction well depth around the cyclopentadienyl ring of ferrocene, as an attractive interaction around 100 meV was calculated for out-of-plane directions of five-membered (furan and thiophene)³³ or six-membered (benzene)³⁴ cyclic aromatic compounds, while a larger well depth (ca. 300 meV) was calculated for the pyrrole–Li system.³³ This difference among cyclic aromatic compounds can be related to the out-of-plane extension of lone-pair electrons belonging to the NH group of pyrrole.

Band 8 shows enhanced intensity in PIES and was assigned mainly to four valence MOs by the ADC(3) calculation.⁵ Although the corresponding MOs have σ_{CH} character, most of them have in-phase extending distributions outside the repulsive surface (molecular surface^{9,18}) within a cyclopentadienyl ring or between two cyclopentadienyl rings. This in-phase extension of MOs results in relatively large ionization probability in Penning ionization because of the large overlapping between the 1s orbital of He* and the target MO. In Figure 2, the orbital character is shown as σ_{CH} , σ_{Cp} for band 8. The small negative CEDPICS ($m = -0.13$) is due to repulsive interaction around the σ_{CH} orbital region and 0° access of Li to the Fe atom in Figure 4.

Structures for bands 7 and 8 are shown in CERPIES (Figure 3) as a–d and a'–g', respectively. In band 7, negative collision energy dependence was obtained for band components b and d, which may be assigned to splitting of ionization from $7a_1'$ (π_{Cp}) as suggested by the ADC(3) calculation.⁵ On the other hand, the structure of band 8 (a'–g') should be assigned to seven or more splitting components. The calculated ionic states at 17–18.5 eV in IP are, however, more than ten by the ADC(3) calculation.⁵ Observed large negative collision energy dependence of a', c', and f' components may be related to ionization from $6e_1'$ (π_{Cp} , 17.28 eV), $4e_1''(d_{xz}, d_{yz} + \pi_{Cp}$, 17.30 eV), and $6a_2''$ (π_{Cp} , 18.49 eV) MOs as suggested by the ADC(3) calculation.⁵

Strong low electron energy band ($E_c < 1$ eV) was observed in PIES. Ionization energy of doubly charged $Fe(Cp)_2^{2+}$ was

TABLE 1: Ionization Potentials (eV) by He I UPS and Theoretical Calculations, Band Assignments, and Slope Parameter (*m*, See Text) of CEDPICS for Ferrocene

band	IP	state	Koopmans ^a	SAC-CI ^b	ADC(3) ^c	P3 ^d	<i>m</i>
1	6.90	² E ₂ '	11.50 (4e ₂ ', d _{xy} , d _{x²-y²})	6.26 (0.747) ^e	7.85 (0.71)		-0.25
2	7.20	² A ₁ '	13.80 (8a ₁ ', d _{z²})	7.27 (0.747) ^f	9.36 (0.58)		-0.29
3	8.76	² E ₁ '	9.29 (6e ₁ ', π _{Cp})	8.78 (0.959)	8.70 (0.90)	9.21 (0.90)	-0.28
4	9.40	² E ₁ ''	9.27 (4e ₁ '', d _{xz} , d _{yz} + π _{Cp})	9.05 (0.960)	9.08 (0.87)	9.72 (0.89)	-0.39
S ₁	(11.0)				10.84 (8a ₁ '(0.06)), 10.92 (4e ₂ '(0.02))		
5	11.90	² A ₂ ''	13.40 (6a ₂ '', π _{Cp})	11.86 (0.919)	12.13 (0.84)	12.19 (0.86)	-0.22
6	12.4	² E ₂ '	14.37 (3e ₂ ', σ _{CH})	12.63 (0.960)	13.08 (0.85)	13.05 (0.90)	-0.15
		² E ₂ ''	14.11 (3e ₂ '', σ _{CH})	12.65 (0.944)	12.96 (0.91)	12.77 (0.89)	
7	13.3	² A ₁ '	15.35 (7a ₁ ', π _{Cp})	13.34 (0.920)	13.71 (0.65)	13.79 (0.85)	-0.21
		² E ₁ '	15.04 (5e ₁ ', σ _{CH})	13.46 (0.978)	13.89 (0.91)	13.54 (0.89)	
		² E ₁ ''	15.14 (3e ₁ '', σ _{CH})	13.69 (0.958)	14.07 (0.88)	13.74 (0.89)	
S ₂	(15.8)	² A ₁ '			16.57 (8a ₁ '(0.05), 6a ₁ '(0.05))		-0.15
8	17.0	² A ₂ ''	18.89 (5a ₂ '')		17.39 (0.81)	16.94 (0.86)	-0.13
		² A ₁ '	19.64 (6a ₁ '')		17.80 (0.68), 16.57 (0.04)	17.78 (0.90)	
		² E ₂ ''	19.86 (2e ₂ '')		17.92 (0.34), 17.94 (0.26)	17.53 (0.85)	
		² E ₂ '	20.23 (2e ₂)		18.22 (0.38)	17.92 (0.86)	

^a MO labels are shown in parentheses. ^b Reference 6. Intensities are shown in parentheses, and half-intensities are shown for e symmetric orbitals. ^c Reference 5. Pole strength values are shown in parentheses. Important lines are selected. ^d Pole strength values are shown in parentheses. ^e Mixing of direct and shake-up configurations was obtained for ²E₂' (0.85(4e₂') + 0.39(4e₁'', 4e₂' → 9e₁'')) state in ref 6. ^f Mixing of direct and shake-up configurations was obtained for ²A₁' (0.82(8a₁') + 0.41(4e₁'', 8a₁' → 9e₁'')) state in ref 6.

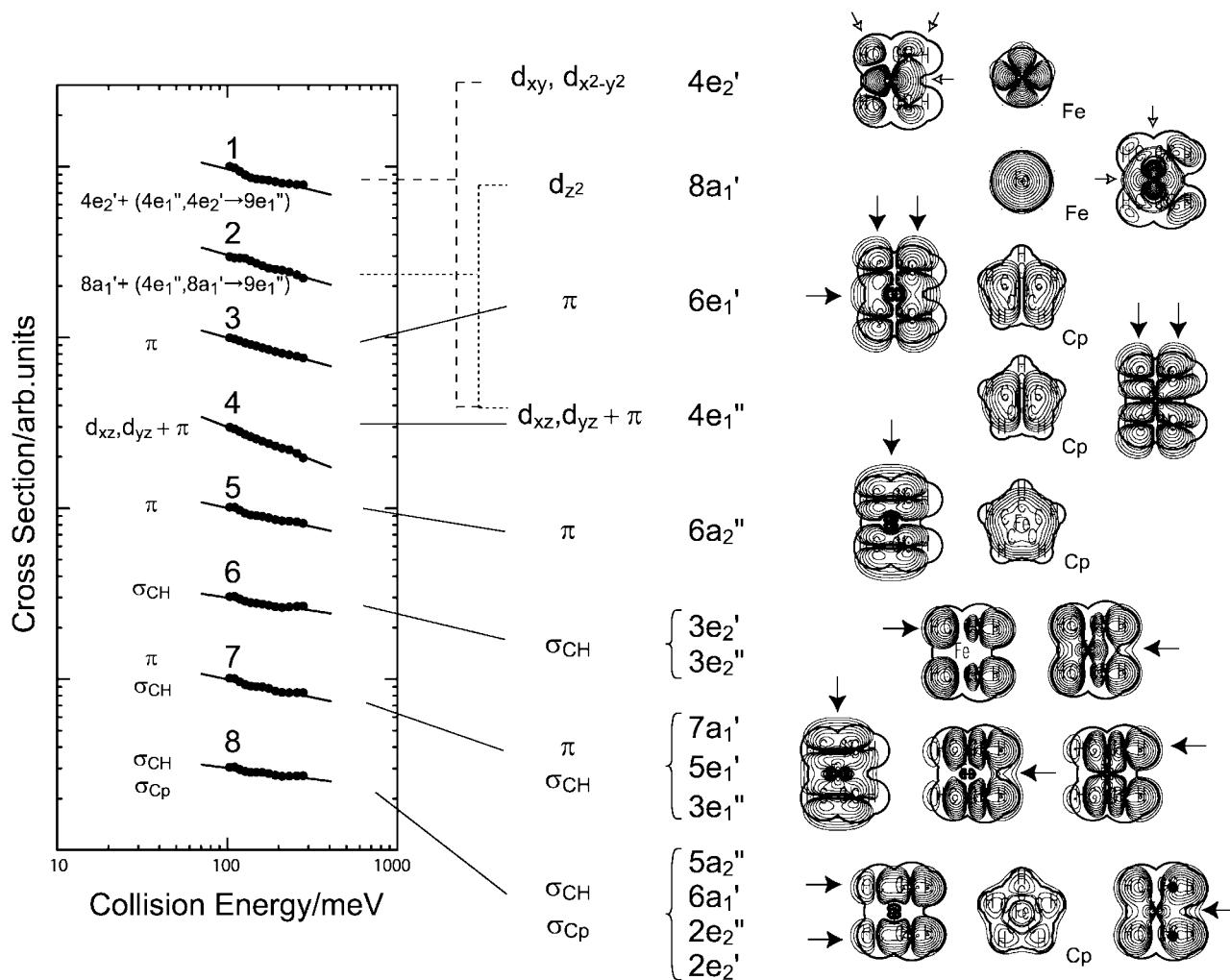


Figure 2. Collision energy dependence of partial ionization cross sections (CEDPICS) of ferrocene by collision with He*(²3S) atoms. Contour maps of electron densities for metal d and ligand valence MOs are also illustrated. Bands 1 and 2 can be assigned to mixing configurations for ²E₂' (4e₂'⁻¹ + (4e₁'', 4e₂' → 9e₁'')) and ²A₁' (8a₁'⁻¹ + (4e₁'', 8a₁' → 9e₁'')) states, respectively (ref 6). Arrows in the figure indicate the most effective directions of collision. Fe and Cp indicate electron density maps on the planes at the Fe atom and 0.85 Å above the Cp ring, respectively.

calculated by the energy difference between doubly ionized and neutral ferrocene molecules with the DFT(B3LYP) method. The lowest triplet state of Fe(Cp)₂²⁺ (19.12 eV) is accessible within

the excitation energy (19.82 eV) of He*(²3S). The shake-up and shake-off satellite may have a relationship with the strong background signals less than *E_c* ≈ 1 eV in PIES.

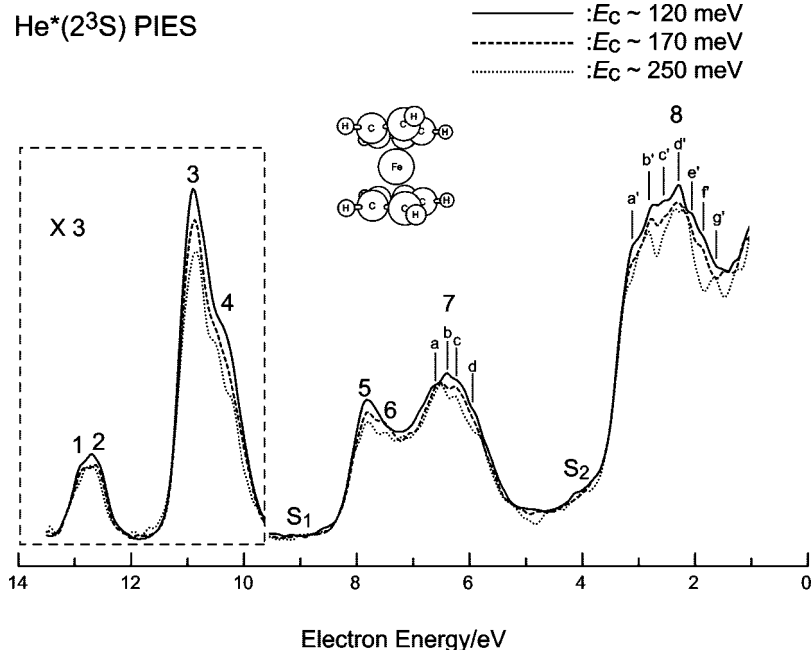


Figure 3. Collision-energy-resolved Penning ionization electron spectra (CERPIES) of ferrocene. Cold spectrum ($E_c \approx 120$ meV), middle spectrum ($E_c \approx 170$ meV), and hot spectrum ($E_c \approx 250$ meV) are shown by solid, dashed, and dotted curves, respectively. The intensity of bands 1–4 is shown 3 times as large as the original one. Structures observed in bands 7 and 8 are denoted as a–d and a'–g', respectively. S_1 and S_2 indicate satellite bands.

It should be noted that the ADC(3) calculation resulted in splitting of ionization bands with small pole strengths for $6a_1'$, $2e_2''$, and $2e_2'$ MOs. In this connection, small bands (S_2) in PIES around 4 eV in E_c (IP ≈ 15.8 eV) may be assigned to satellite bands for ionization from $8a_1'$ and $6a_1'$ MOs according to the ADC(3) calculation,⁵ which is consistent with the small negative collision energy dependence in CEDPICS ($m = -0.15$) and CERPIES for band S and repulsive interaction around the $6a_1'$ (Fe) and $8a_1'$ (σ_{CH}) MO region.

B. Ionization from Metal d Orbitals. The most negative slope value of CEDPICS ($m = -0.39$) was observed for ionization from the $4e_1''$ ($d_{xz}, d_{yz} + \pi_{Cp}$) orbital (band 4). For this $4e_1''$ orbital, cyclopentadienyl π components are in-phase with the metal d_{xz}, d_{yz} orbitals and out-of-phase around the Fe atom, which results in the largest negative slope value of CEDPICS reflecting the attractive interaction for the π direction access (90° in Figure 4). The difference in slope values of CEDPICS for band 3 ($6e_1'$, $m = -0.28$) and band 4 ($4e_1''$, $m = -0.39$) can be attributed to the repulsive interaction around the Fe atom for ionization from the $6e_1'$ MO.

For bands 1 and 2 in PIES, the obtained slope values of CEDPICS are relatively negatively large ($m = -0.25, -0.29$). The extending electron densities of $4e_2'$ and $8a_1'$ MOs are small and similar around the Fe atom (Figure 2), and interaction potential around the Fe atom is repulsive due to shielding by Cp rings, which is inconsistent with the obtained negative CEDPICS for bands 1 and 2. Although small electron densities of $4e_2'$ and $8a_1'$ MOs above the Cp rings (in attractive area) may contribute to the observed bands 1 and 2 in some degree, this inconsistency should be discussed on the strong electron correlation effects in ionization. The recent ab initio MO calculation for cationic states of ferrocene by SAC/SAC-CI theory⁶ indicated that the first two ionic states can be represented by strong mixing of direct and shake-up ionization configurations with the $4e_1''$ MO (${}^2E_2'$: $0.85(4e_2') + 0.39(4e_1'', 4e_2' \rightarrow 9e_1'')$), ${}^2A_1'$: $0.82(8a_1') + 0.41(4e_1'', 8a_1' \rightarrow 9e_1'')$). In addition, strong electron correlation effects for these first two ionic states can

be inferred from the small pole strength values for ionization from $4e_2'$ (0.71) and $8a_1'$ (0.58) MOs by ADC(3) calculation.⁵ In the case of the P3 calculation, a reasonable result was not obtained only for ionization from these two MOs. Thus, the negative CEDPICS for bands 1 and 2 can be related to the ionization from $4e_1''$ ($d_{xz}, d_{yz} + \pi_{Cp}$) MO and the attractive interaction above the Cp ring. In this relationship, it should be noted that negative slopes of CEDPICS for shake-up bands accompanying π - π^* excitation were observed in PIES of benzene^{34,35} and five-membered cyclic aromatic compounds.³³ Small satellite bands were observed in UPS and PIES at IP ≈ 11 eV denoted as S_1 . According to the ADC(3) calculation,⁵ this small band can be ascribed to ionization from $4e_2'$ ($d_{xy}, d_{x^2-y^2}$) and $8a_1'$ (d_{z^2}) MOs. The small intensity of this S_1 band in PIES can be consistent with the small extension of the electron density for $4e_2'$ ($d_{xy}, d_{x^2-y^2}$) and $8a_1'$ (d_{z^2}) MOs as shown in Figure 2.

Regarding the intensity of bands 1 and 2 in PIES, band 2 has much larger (nearly two times) intensity than band 1.¹¹ The transition probability P is proportional to the square of the matrix elements between the initial state wave function Φ_i and final ionic state wave function Φ_f , and it can be expressed as

$$P \approx |\langle \Phi_f | r_{12}^{-1} | \Phi_i \rangle|^2 \quad (3)$$

where r_{12}^{-1} is the electronic interaction operator. For the final state, the wave function Φ_f is the summation of direct and shake-up ionization configurations for ${}^2E_2'$ ($(4e_2') + (4e_1'', 4e_2' \rightarrow 9e_1'')$) or ${}^2A_1'$ ($(8a_1') + (4e_1'', 8a_1' \rightarrow 9e_1'')$) state⁶ with a ground state He atom and an outgoing electron. When the MOs are those of isolated systems, the shake-up configurations do not yield nonvanishing contributions to P . However, if the orbital distortion upon Penning ionization occurs due to the interaction with the neighboring helium atom or some other reason, the shake-up configurations become nonvanishing terms. Since coefficients in the configuration interaction for the ${}^2E_2'$ state ($0.85(4e_2') + 0.39(4e_1'', 4e_2' \rightarrow 9e_1'')$) and the ${}^2A_1'$ state ($0.82(8a_1') + 0.41(4e_1'', 8a_1' \rightarrow 9e_1'')$)⁶ are similar, the intensity difference

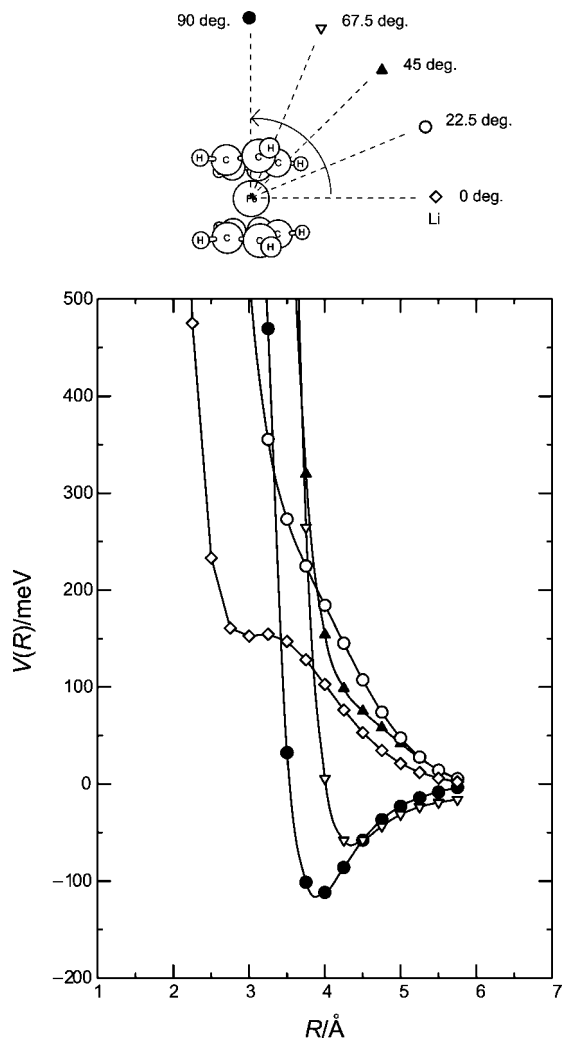


Figure 4. Interaction potential energy curves $V(R)$ by B3LYP/6-311+G* calculations as a function of distance R between Fe and Li for the access directions of 0° , 22.5° , 45° , 67.5° , and 90° .

in PIES for bands 1 and 2 may indicate the larger degree of orbital distortion for d_{z^2} ($8a_1'$) MO rather than for d_{xy} , $d_{x^2-y^2}$ ($4e_2'$) MO around the Cp rings accompanying with $d-d^*$ ($9e_1''$) excitation upon ionization.

IV. Conclusion

Penning ionization of ferrocene with $\text{He}^*(2^3\text{S})$ metastable atoms was observed by collision-energy-resolved two-dimensional electron spectroscopy. Collision energy dependence of partial ionization cross section (CEDPICS) for each ionic state indicates that strong attractive interaction around the cyclopentadienyl rings (Cp) results in a negative slope of CEDPICS for ionization from valence π_{Cp} orbitals. Repulsive interaction was also found around the σ_{CH} bonds and the Fe atom. The small band structure in CERPIES can be related to satellite bands suggested by a Green's functional method including electron correlation effects (ADC(3)).⁵

A negative CEDPICS of bands 1 and 2 was ascribed to strong electron correlation effects in mixing configurations of direct ionization from metal d orbitals and shake-up ionization

accompanied by $d-d^*$ transition as shown by CI calculation (SAC/SAC-CI).⁶ Information on strong electron correlation effects in ionic states of other organometallic compounds may be obtained by 2D Penning ionization electron spectroscopy.

Acknowledgment. This research was supported by a Grant for Scientific Research from the Ministry of Education, Culture, Sport, Science, and Technology (MEXT) of Japan. The authors thank Prof. Hideo Yamakado in Wakayama University for providing valuable comments on the experiment in this study.

References and Notes

- (1) Kealy, T. J.; Paulson, P. L. *Nature (London)* **1951**, *168*, 1039.
- (2) Rabalais, J. W.; Werme, L. O.; Bergmark, T.; Karlsson, L.; Hussain, M.; Siegbahn, K. *J. Chem. Phys.* **1972**, *57*, 1185.
- (3) Evans, S.; Green, M. L. H.; Jewitt, B.; Orchard, A. F.; Pygall, C. F. *J. Chem. Soc., Faraday II* **1972**, *68*, 1847.
- (4) Cautelli, C.; Green, J. C.; Kelly, M. R.; Powell, P.; Tilberg, J. V.; Robbins, J.; Smart, J. *J. Electron Spectrosc. Relat. Phenom.* **1980**, *19*, 327.
- (5) Ohno, M.; von Niessen, V.; Schüle, J. *J. Chem. Phys.* **1991**, *158*, 1.
- (6) Ishimura, K.; Hada, M.; Nakatsuji, H. *J. Chem. Phys.* **2002**, *117*, 6533.
- (7) Cooper, G.; Green, J. C.; Payne, M. P. *Mol. Phys.* **1988**, *63*, 1031.
- (8) von Wald, G. A.; Taylor, J. W. *J. Electron Spectrosc. Relat. Phenom.* **1988**, *47*, 315.
- (9) Ohno, K.; Mutoh, H.; Harada, Y. *J. Am. Chem. Soc.* **1983**, *105*, 4555.
- (10) Munakata, T.; Harada, Y.; Ohno, K.; Kuchitsu, K. *Chem. Phys. Lett.* **1981**, *84*, 6.
- (11) Masuda, S.; Aoyama, M.; Harada, Y. *J. Am. Chem. Soc.* **1990**, *112*, 6445.
- (12) Mutoh, H.; Masuda, S. *J. Chem. Soc., Dalton Trans.* **2002**, 1875.
- (13) Harada, Y.; Ohno, K.; Mutoh, H. *J. Chem. Phys.* **1983**, *79*, 3251.
- (14) Masuda, S.; Harada, Y. *J. Chem. Phys.* **1992**, *96*, 2469.
- (15) Ohno, K.; Yamakado, H.; Ogawa, T.; Yamata, T. *J. Chem. Phys.* **1996**, *105*, 7536.
- (16) Kishimoto, N.; Ohno, K. *Int. Rev. Phys. Chem.* **2007**, *26*, 93.
- (17) Ohno, K.; Takami, T.; Mitsuke, K.; Ishida, T. *J. Chem. Phys.* **1991**, *94*, 2675.
- (18) Ohno, K. *Bull. Chem. Soc. Jpn.* **2004**, *77*, 887.
- (19) Takami, T.; Mitsuke, K.; Ohno, K. *J. Chem. Phys.* **1991**, *95*, 918.
- (20) Gardner, J. L.; Samson, J. A. R. *J. Electron Spectrosc. Relat. Phenom.* **1976**, *8*, 469.
- (21) Kimura, K.; Katsumata, S.; Achiba, Y.; Yamazaki, T.; Iwata, S. *Handbook of He I Photoelectron Spectra of Fundamental Organic Molecules*; Japan Scientific Societies Press: Tokyo, Japan, 1981.
- (22) Kishimoto, N.; Aizawa, J.; Yamakado, H.; Ohno, K. *J. Phys. Chem. A* **1997**, *101*, 5038.
- (23) (a) Böhn, R. K.; Haaland, A. *J. Organomet. Chem.* **1968**, *5*, 470. (b) Haaland, A.; Nilsson, J. E. *Acta Chem. Scand.* **1968**, *22*, 2653. (c) Orsenblum, M. *Chemistry of Iron Group Metallocenes*; Interscience: New York, 1965; Chapter 3, Part I.
- (24) Pauling, L. *The Nature of the Chemical Bond*; Cornell University Press: Ithaca, NY, 1960.
- (25) Ortiz, J. V. *J. Chem. Phys.* **1996**, *104*, 7599.
- (26) Frisch, M. J.; et al. *GAUSSIAN 03*, Revision C.02; Gaussian, Inc., Pittsburgh, PA, 2003.
- (27) Niehaus, A. *Adv. Chem. Phys.* **1981**, *45*, 399.
- (28) Hotop, H.; Roth, T. E.; Ruf, M.-W.; Yench, A. *J. Theor. Chem. Acc.* **1998**, *100*, 36.
- (29) Becke, A. D. *J. Chem. Phys.* **1993**, *7*, 5648.
- (30) Boys, S. F.; Bernardi, F. *Mol. Phys.* **1970**, *19*, 55.
- (31) Ohshimo, K.; Tsunoyama, H.; Yamakita, Y.; Misaizu, F.; Ohno, K. *Chem. Phys. Lett.* **1999**, *301*, 356.
- (32) Hotop, H.; Niehaus, A. *Z. Phys.* **1969**, *228*, 68.
- (33) Kishimoto, N.; Yamakado, H.; Ohno, K. *J. Phys. Chem.* **1996**, *100*, 8204.
- (34) Yamazaki, M.; Kishimoto, N.; Ohno, K. *J. Chem. Phys.* **2005**, *122*, 044303.
- (35) Takami, T.; Ohno, K. *J. Chem. Phys.* **1992**, *96*, 6253.